

# Dissecting Hadrons in Continuum QCD Approach

---

**Adnan Bashir**

Institute of Physics and Mathematics  
University of Michoacán, Morelia, Michoacán, Mexico  
Fulbright Visiting Scientist  
Jefferson Laboratory, Newport News, Virginia, USA



**HUGS2023**

May 30 - June 16, 2023  
Newport News, VA

The 38th Annual Hampton University Graduate Summer Program at Jefferson Lab

**Jefferson Lab**  
Exploring the Nature of Matter

# QCD: Facts and Challenges

QCD is characterized by two **emergent** phenomena: **confinement** and dynamical generation of mass (**DGM**).

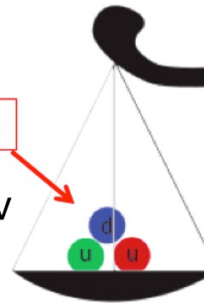
$$\mathcal{L}_{\text{QCD}} = \sum_{j=u,d,s,\dots} \bar{q}_j [\gamma_\mu D_\mu + m_j] q_j + \frac{1}{4} G_{\mu\nu}^a G_{\mu\nu}^a,$$
$$D_\mu = \partial_\mu + ig \frac{1}{2} \lambda^a A_\mu^a,$$
$$G_{\mu\nu}^a = \partial_\mu A_\nu^a - \partial_\nu A_\mu^a - gf^{abc} A_\mu^b A_\nu^c,$$

- Quarks and gluons do not reach detectors.
- Formation of color-singlet bound states: “**Hadrons**” mesons, baryons, tetraquarks, molecules
- Emergence of hadron masses (**EHM**) from QCD **dynamics**



Higgs mechanism

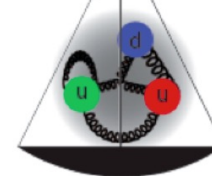
Quark Mass ~ 3 MeV



~ 1% of proton mass

Dynamics of gluons

Proton Mass = 938.27 MeV



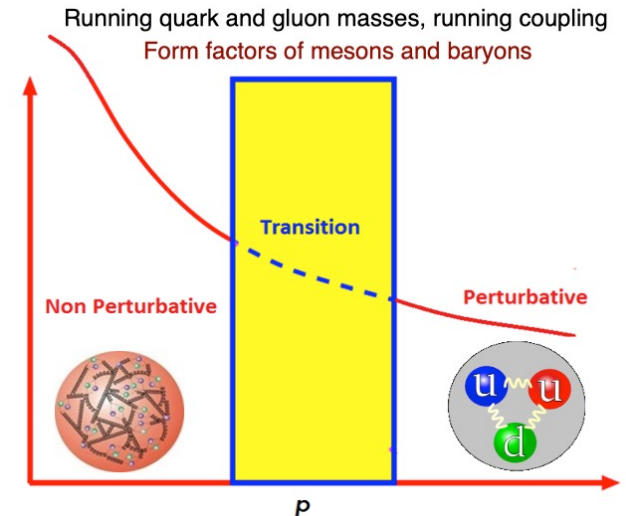
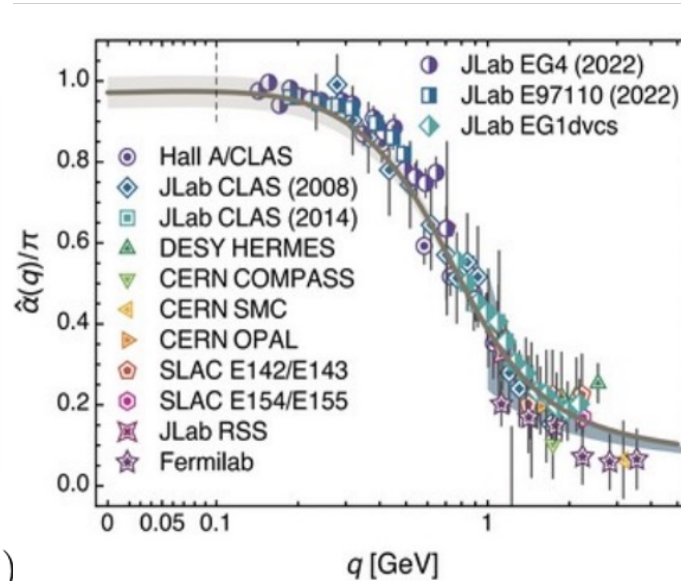
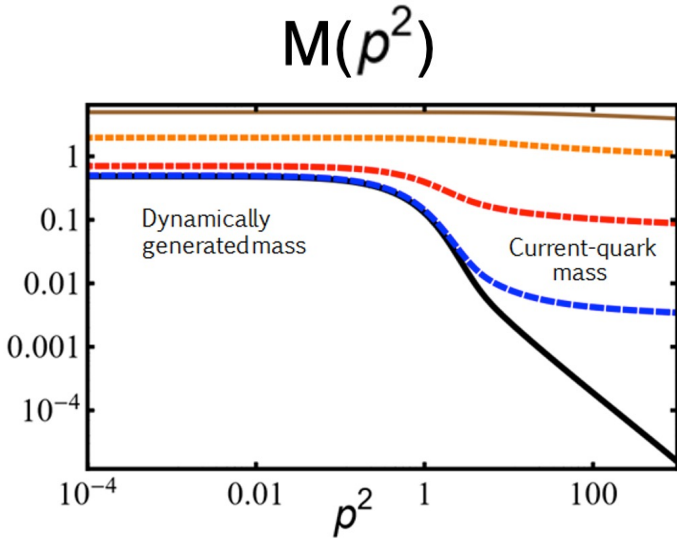
~ 99% of proton mass

# QCD: Current Understanding and Challenges

Origins of **confinement** and **dynamical mass generation** can be traced back to the Green functions of **quarks** and **gluons**.

These emergent phenomena of **QCD**, non-existent in perturbation theory are naturally linked to the infrared enhancement of the **strong running coupling**.

The effects of the pattern of **dynamical mass generation** are traceable in the  **$Q^2$  evolution** of the **meson** and **baryon form factors** explored and planned in the **JLab** and the **EIC**.

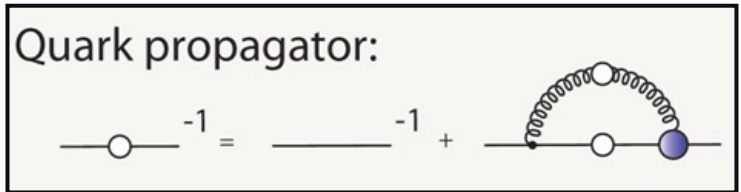


$$S_f^{-1}(p) = Z_f^{-1}(p^2)(i\gamma \cdot p + \mathbf{M}_f(p^2))$$

# QCD – Schwinger-Dyson Equations

## Gauge Technique – Non Perturbative Solutions

- A. Salam, R. Delbourgo, Phys. Rev. 135 (1964) 6, B1398-B1427.  
DCSB - Non-perturbative QED
- P.I. Fomin, V.A. Miransky, Phys. Lett. B64 (1976) 166-168.  
DCSB – Non-abelian Gauge Theories
- V. Miransky, V. Gusynin, Y. Sitenko, Phys. Lett. B100 (1981) 157-162  
DCSB – MT Model - Vector Mesons
- P. Maris, P. Tandy, Phys. Rev. C60 (1999)



$$S(p^2, \mu^2) = \frac{Z(p^2, \mu^2)}{i \gamma \cdot p + M(p^2)}$$

PHYSICAL REVIEW VOLUME 135, NUMBER 6B 21 SEPTEMBER 1964

### Renormalizable Electrodynamics of Scalar and Vector Mesons. II

ABDUS SALAM\*  
*Imperial College, London, England*

ROBERT DELBOURGO†  
*Imperial College, London, England*

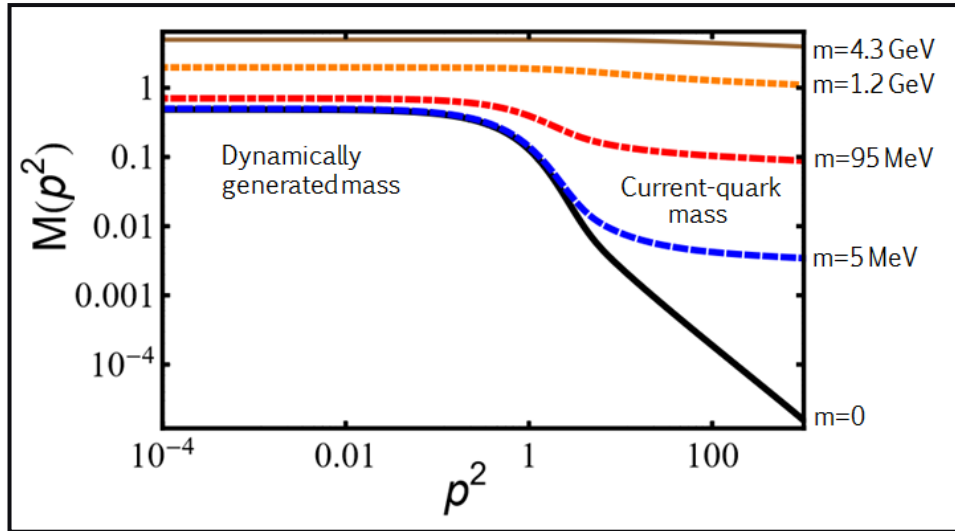
The "gauge technique" for solving field theories introduced in an earlier paper is applied to scalar and vector electrodynamics.

A. Dyson-Schwinger Set;

For a typical 3-field (e.g., electron-photon) interaction the well-known Dyson equations

$$S^{-1} = Z_2 S_0^{-1} + Z_1 e^2 \int \Gamma S \Gamma_0 D \quad \leftarrow \text{(I.1)}$$

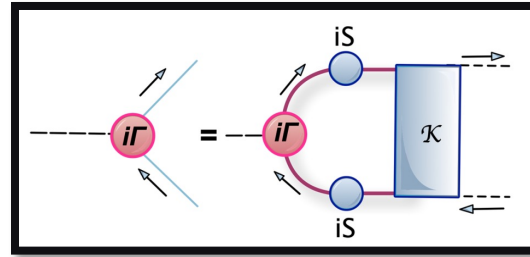
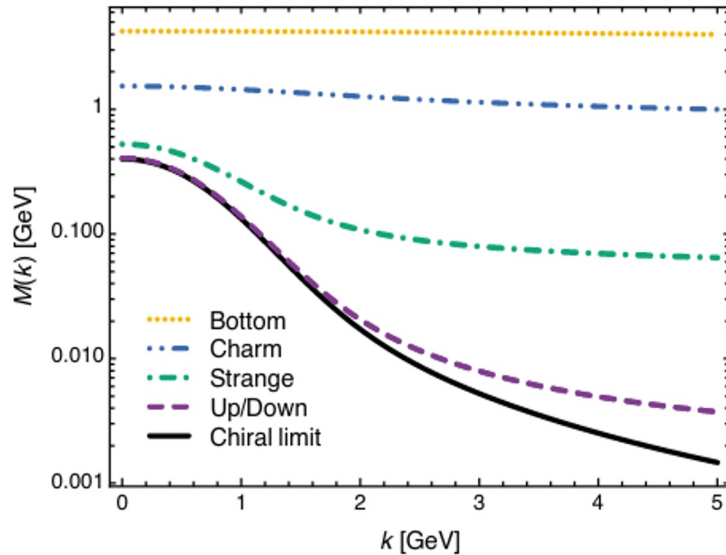
SDE: electron propagator

$$D^{-1} = Z_3 D_0^{-1} + Z_1 e^2 \int \Gamma S \Gamma_0 S \quad \text{(I.2)}$$


# $\pi$ : Bound State and Goldstone Boson

The pattern of **dynamical chiral symmetry breaking** and the **Bethe-Salpeter amplitude** to be computed by solving the **Bethe-Salpeter equation**.

$$\Gamma_\pi(k, P) = \gamma_5 \left[ iE_\pi(k; P) + \gamma \cdot P F_\pi(k; P) + \gamma \cdot k k \cdot P G_\pi(k; P) + \sigma_{\mu\nu} k_\mu P_\nu H_\pi(k; P) \right]$$



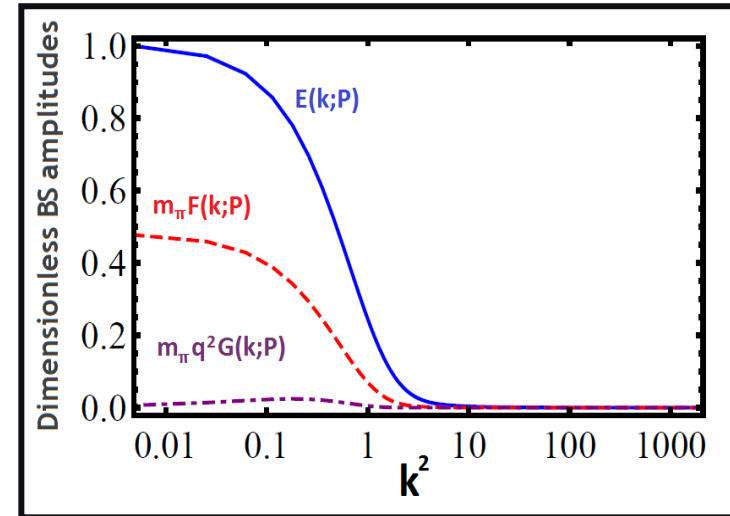
$$S(p) = \frac{1}{i\gamma \cdot p A(p^2) + B(p^2)}$$

$$f_\pi E_\pi(k; P=0) = B(p^2)$$

$$F_R(k; 0) + 2 f_\pi F_\pi(k; 0) = A(k^2)$$

$$G_R(k; 0) + 2 f_\pi G_\pi(k; 0) = 2A'(k^2)$$

$$H_R(k; 0) + 2 f_\pi H_\pi(k; 0) = 0$$



# $\pi$ : Probing Quarks with Photons

In studying the **elastic form factors**, it is the **photon** which probes the **dressed quarks** inside the **bound states**, highlighting the importance of the **quark-photon vertex**.

Gauge covariance  
(WTI, TTI, LKFT),  
kinematic singularities,  
perturbation theory,  
multiplicative  
renormalizability

$$\Gamma_{\mu}^L(p, k, q) = \sum_{i=1}^4 \lambda_i L_{\mu}^i(p, k)$$

$$L_{\mu}^1 = \gamma_{\mu}$$

$$L_{\mu}^2(p, k) = (\not{p} + \not{k})(p + k)_{\mu}$$

$$L_{\mu}^3(p, k) = -(p + k)_{\mu}$$

$$L_{\mu}^4(p, k) = -\sigma_{\mu\nu}(p + k)^{\nu}$$

$$\Gamma_{\mu}^T(p, k, q) = \sum_{i=1}^8 \tau_i(p^2, k^2, q^2) T_{\mu}^i(p, k)$$

$$T_{\mu}^1 = p_{\mu}(k \cdot q) - k_{\mu}(p \cdot q),$$

$$T_{\mu}^2 = [p_{\mu}(k \cdot q) - k_{\mu}(p \cdot q)] (\not{p} + \not{k}),$$

$$T_{\mu}^3 = q^2 \gamma_{\mu} - q_{\mu} \not{q},$$

$$T_{\mu}^4 = q^2 [\gamma^{\mu} (\not{k} + \not{p}) - (k + p)^{\mu}]$$

$$+ 2(k - p)^{\mu} \sigma_{\nu\lambda} p^{\nu} k^{\lambda},$$

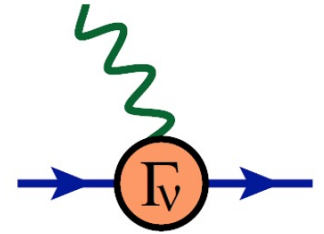
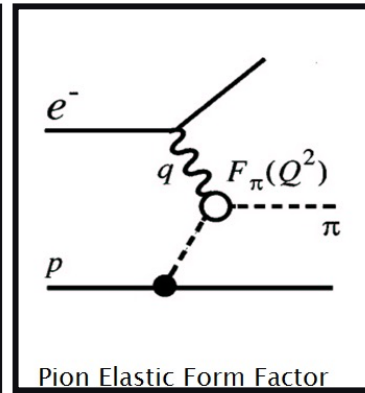
$$T_{\mu}^5 = -\sigma_{\mu\nu} q^{\nu},$$

$$T_{\mu}^6 = \gamma_{\mu}(p^2 - k^2) + (p + k)_{\mu} \not{q},$$

$$T_{\mu}^7 = \frac{1}{2}(p^2 - k^2) [\gamma_{\mu}(\not{p} + \not{k}) - (p + k)_{\mu}]$$

$$- (p + k)_{\mu} \sigma_{\nu\lambda} p^{\nu} k^{\lambda},$$

$$T_{\mu}^8 = \gamma_{\mu} \sigma_{\nu\lambda} p^{\nu} k^{\lambda} - p_{\mu} \not{k} + k_{\mu} \not{p}.$$



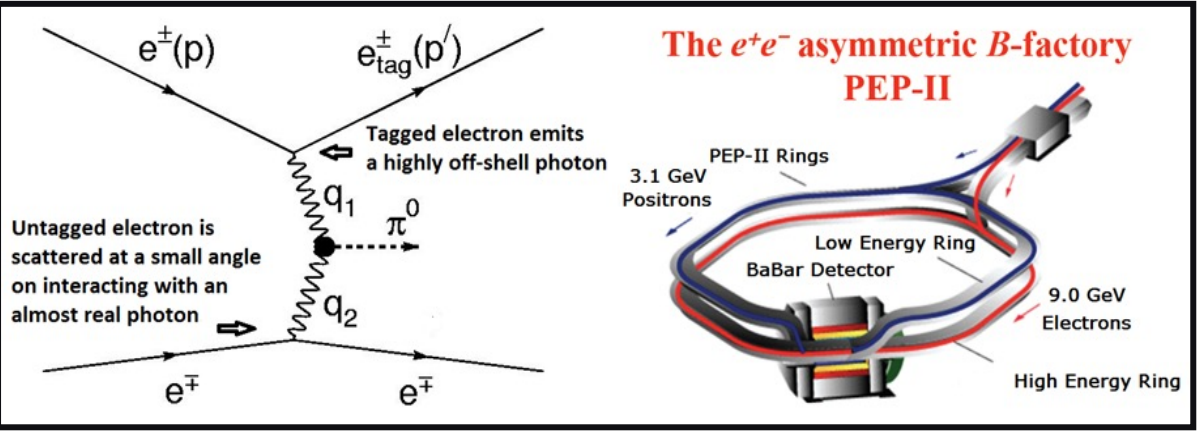
AB, R. Bermudez, L. Chang, C.D. Roberts  
Phys. Rev. C85, 045205 (2012)

L. Albino, AB, L. Gutiérrez, B. El Bennich, E. Rojas  
Phys. Rev. D100 054028 (2019)

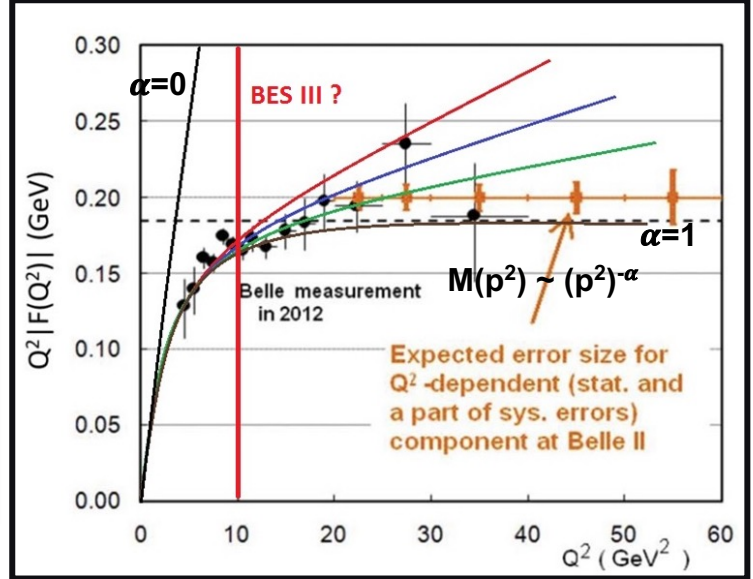
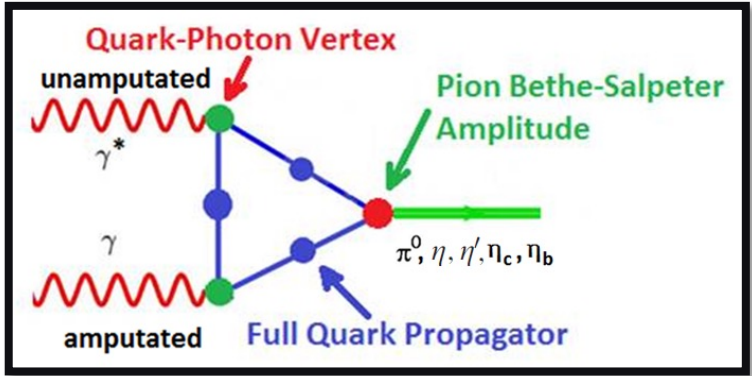
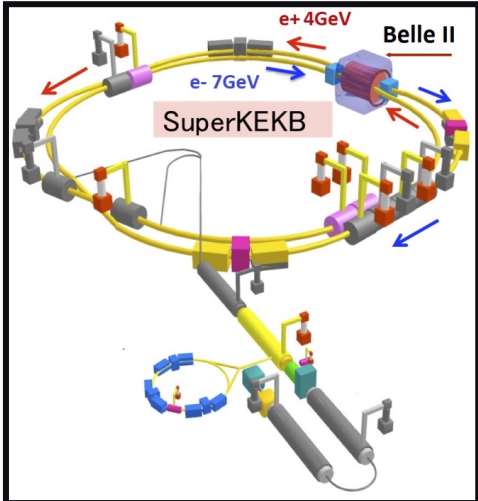
V. Banda, AB, Phys. Rev. D 107 (2023) 7, 073008

J. Roberto Lessa, F. Serna, B. El-Bennich, AB,  
O. Oliveira, Phys. Rev. D 107 (2023) 7, 074017

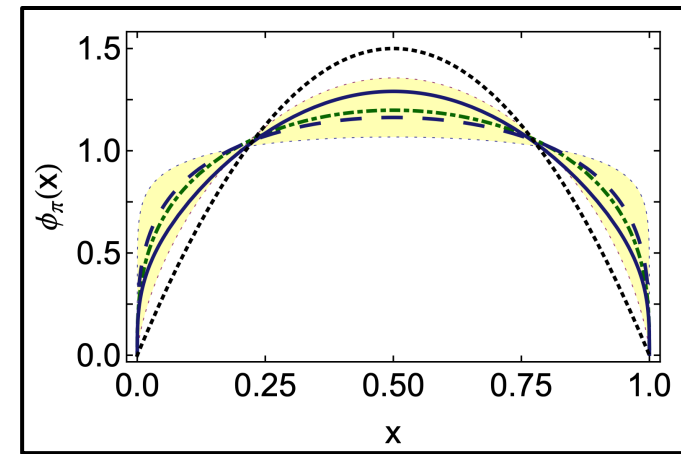
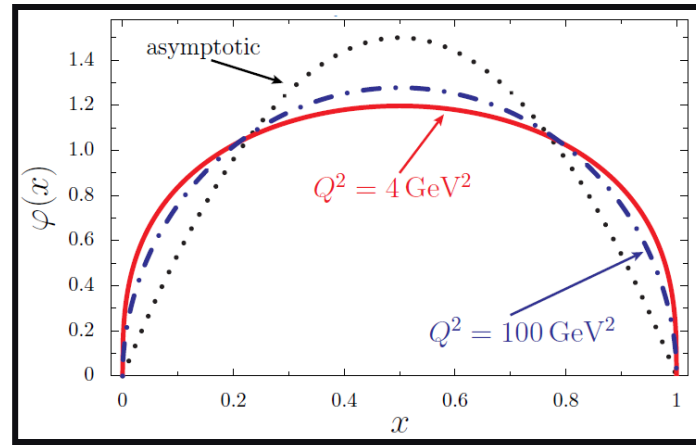
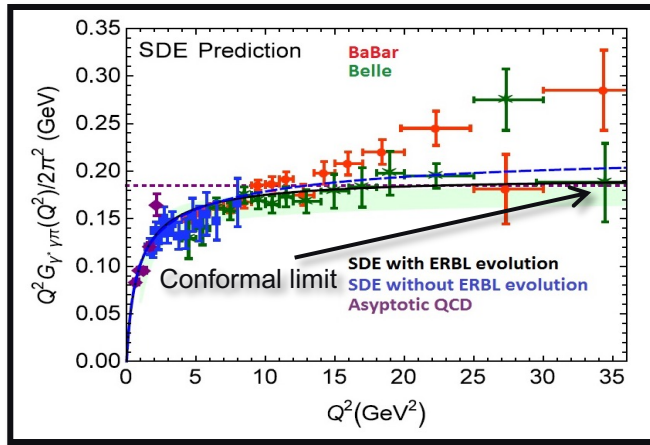
# $\pi^0 \rightarrow \gamma^* \gamma$ Transition Form Factor



The pattern of **dynamical chiral symmetry breaking** dictates the  **$Q^2$  evolution** of the **transition form factor**. Experiment and **asymptotic QCD** for largest  $Q^2$  provide verifications.



# $\pi^0 \rightarrow \gamma^* \gamma$ Transition Form Factor



Satisfies abelian anomaly and agrees with the prediction of **asymptotic QCD**.

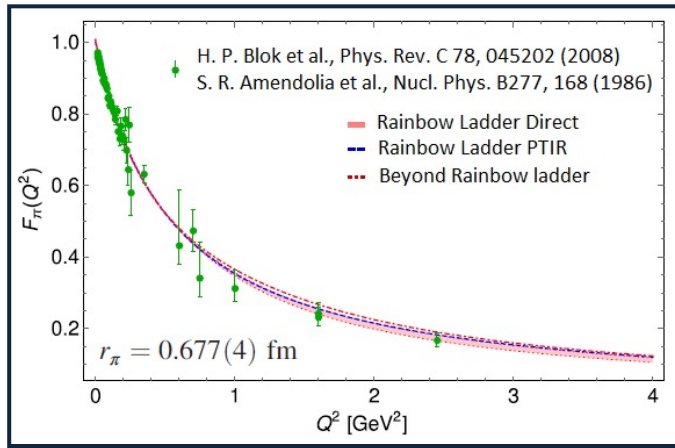
Agrees well with experiment from low to intermediate range of momenta and favors Belle results.

The **distribution amplitude (PDA)** is broad and concave at the **hadronic** scale.

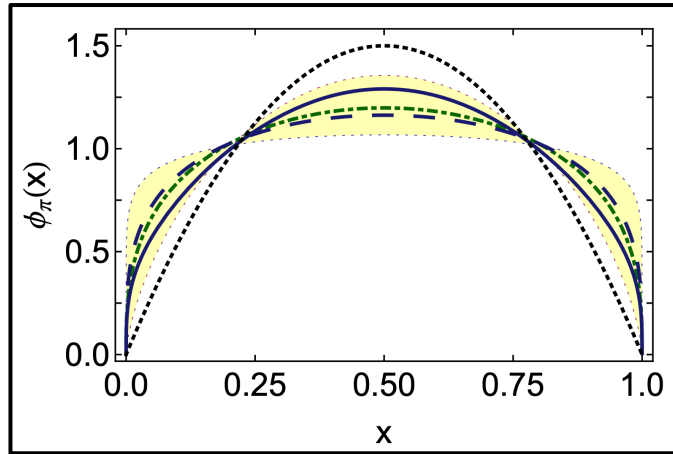
Within an error band stemming from the construction of the **PDA** from the **lattice moments**, it is in good agreement.



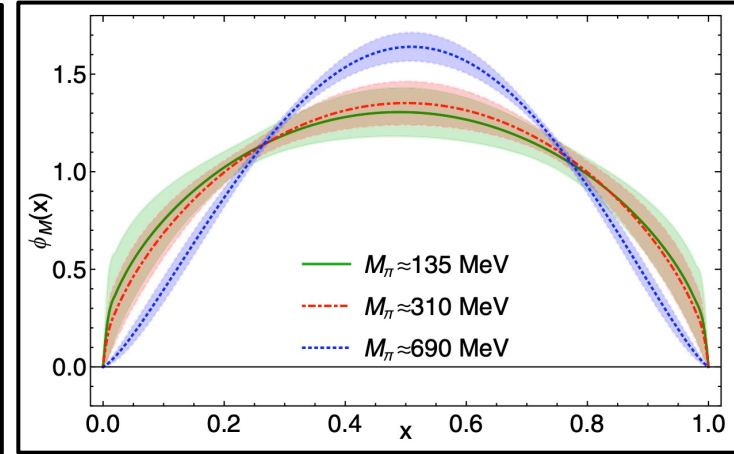
# $\pi$ Electromagnetic Form Factor



A. Miramontes et. al., Phys. Rev. D 105 (2022) 7, 074013



I.C. Cloet, et. al.  
Phys. Rev. Lett. 111 (2013) 092001



R. Zhang, et. al.,  
Phys. Rev. D 102 (2020) 9, 094519

The **electromagnetic form factor** of  $\pi$  is central to the Jlab and planned EIC research.

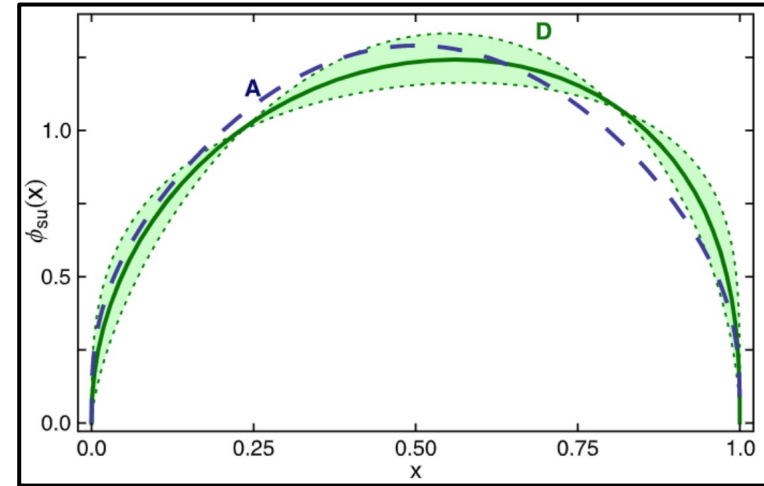
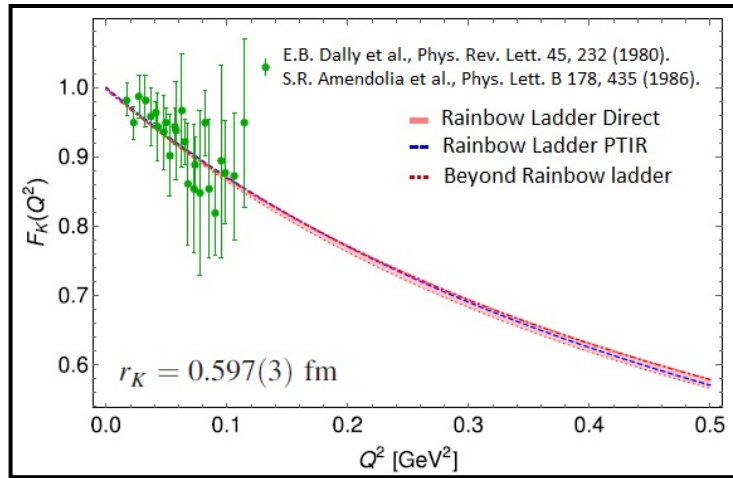
**Jefferson Lab:** Lattice Hadron Physics Collaboration, Frederic D.R. Bonnet, et. al. Phys. Rev. D 72 (2005) 054506

Our computation is consistent with the **valence quark distribution amplitude (PDA)** which is broad and concave at the **hadronic** scale.

The results agree with earlier computation of the **electromagnetic form factors** of  $\pi$ .

L. Chang, I.C. Cloet, C.D. Roberts, S.M. Schmidt, P. Tandy, Phys. Rev. Lett. 111 (2013) 14, 141802

# K Electromagnetic Form Factor



A. Miramontes et. al., Phys. Rev. D 105 (2022) 7, 074013

J. Segovia et. Al. , Phys. Lett. B 731 (2014) 13-18

The **electromagnetic form factors** of  $\pi$  and **K** can be measured till  $Q^2 \sim 8 \text{ GeV}^2$  (10-40  $\text{GeV}^2$ ) and  $5 \text{ GeV}^2$  (10-20  $\text{GeV}^2$ ) respectively in the **12 GeV** upgrade of **JLab (EIC)**.

A. Aguilar, Eur. Phys. J. A55 (2019) 10, 190

The results obtained from the **Schwinger-Dyson equations** appear robust under the calculational scheme employed and ingredients used as in the computation of the **transition form factors** and the **distribution amplitudes** of mesons.

# $\pi$ and $K$ Form Factors: Probing the Standard Model

A muon with spin  $s$  has a **magnetic moment**:  $\mu = g \frac{e}{2m} s$

The factor  $g$  is called the gyro-magnetic factor. The **Dirac equation** for a charged elementary fermion with spin  $1/2$  implies  $g = 2$ .

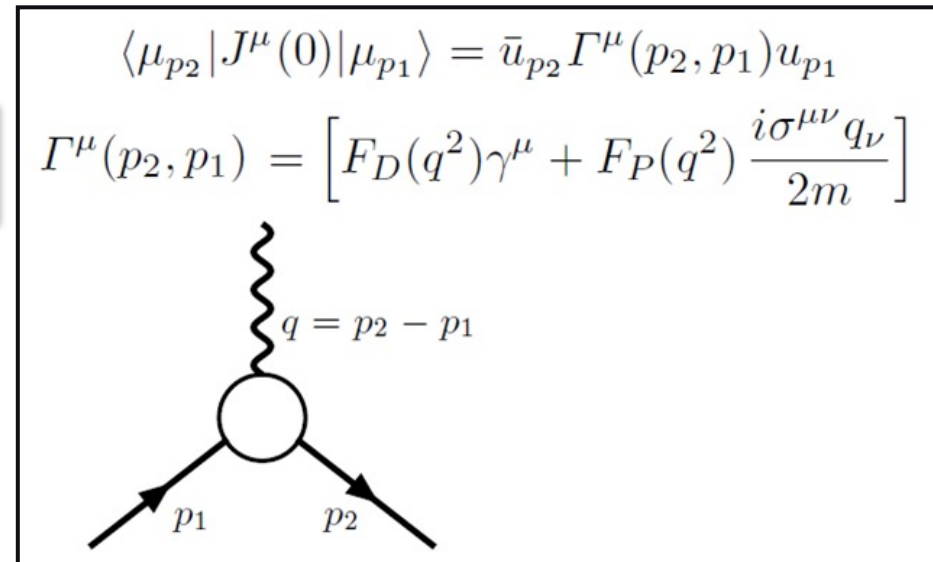
The **anomalous magnetic moment** is the deviation from  $g = 2$ , parameterized by  $a_\mu = (g-2)/2$ . It appears due to radiative corrections. **Renormalization** of **QED** was established in 1943 and 1947-1948 by Tomonaga, Schwinger and Feynman.

The leading contribution to  $a_\mu$ , calculated by Schwinger in 1949, is:

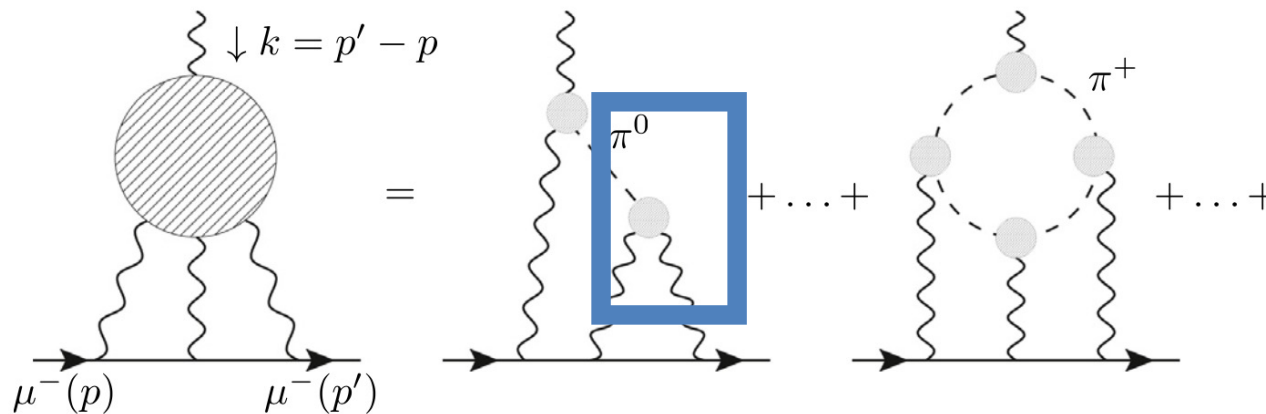
$$a_\mu = \frac{\alpha}{2\pi}$$

The **amplitude** of a muon scattering off an external electromagnetic field  $A$  is: ( $q=p_2-p_1$ ):

$$\mathcal{M} = -ie \langle \mu_{p_2} | J^\mu(0) | \mu_{p_1} \rangle A_\mu(q)$$

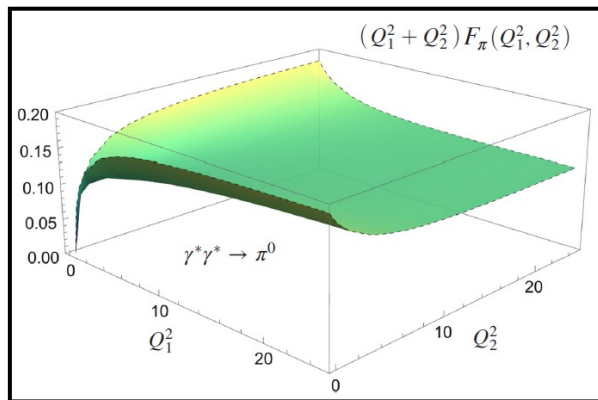
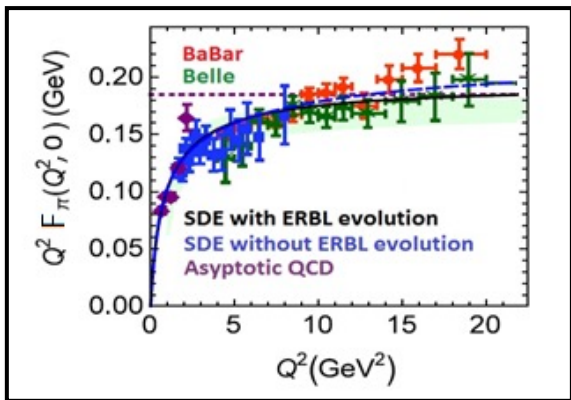


# Neutral Pseudoscalar Pole Contributions



$a_{\mu}^{\pi^0\text{-pole}}$	$= (61.4 \pm 2.1) \times 10^{-11}$
$a_{\mu}^{\eta\text{-pole}}$	$= (14.7 \pm 1.9) \times 10^{-11}$
$a_{\mu}^{\eta'\text{-pole}}$	$= (13.6 \pm 0.8) \times 10^{-11}$
$a_{\mu}^{\eta_c\text{-pole}}$	$= (0.9 \pm 0.1) \times 10^{-11}$
$a_{\mu}^{\eta_b\text{-pole}}$	$= (0.0026 \pm 0.0001) \times 10^{-11}$
$a_{\mu}^{\text{PS-pole}}$	$= (90.6 \pm 4.9) \times 10^{-11}$

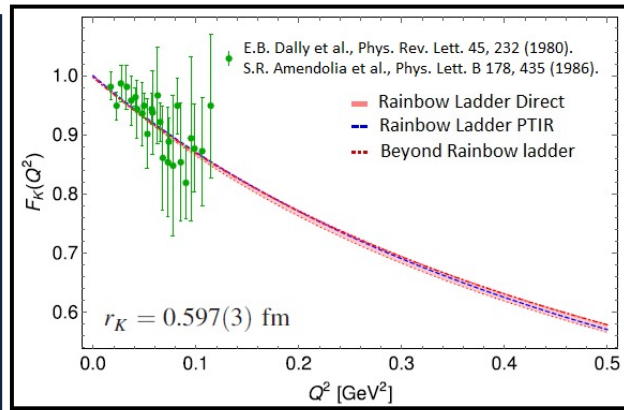
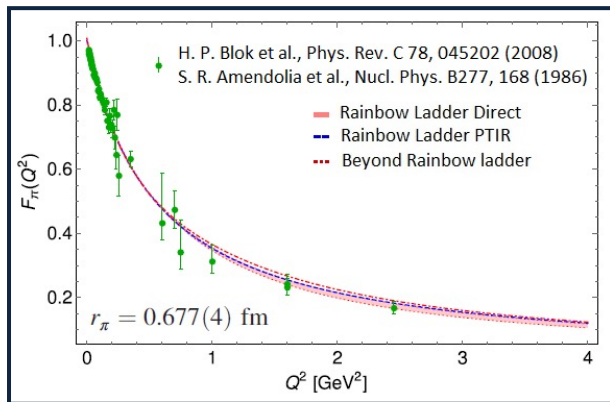
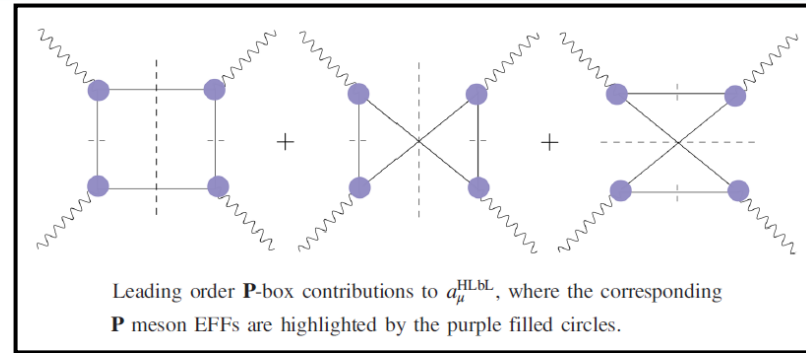
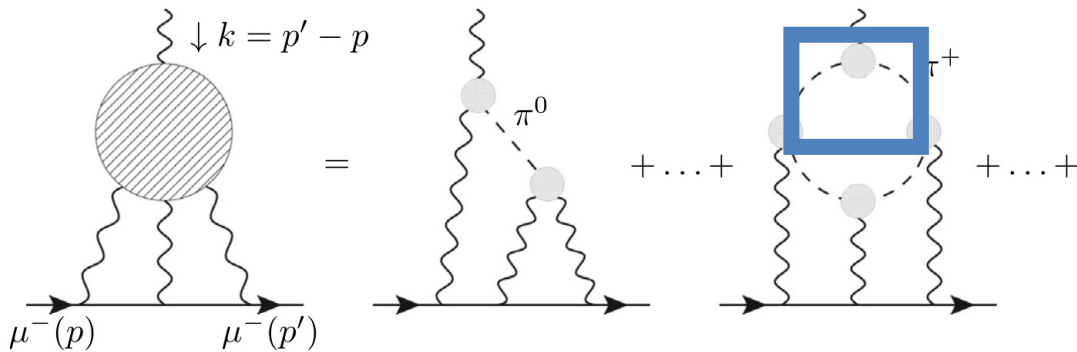
The transition form factor  $\pi^0 \rightarrow \gamma^* \gamma$  extended to  $\pi^0 \rightarrow \gamma^* \gamma^*$ .



Dispersive methods:	$a_{\mu}^{\pi^0\text{-pole}} = 63.6(2.7) \times 10^{-11}$
	$a_{\mu}^{\eta\text{-pole}} = 16.3(1.4) \times 10^{-11}$
	$a_{\mu}^{\eta'\text{-pole}} = 14.5(1.9) \times 10^{-11}$
Lattice:	$a_{\mu}^{\pi^0\text{-pole}} = 59.7(3.6) \times 10^{-11}$

K. Raya, AB, P. Roig,  
Phys. Rev. D 101 (2020) 7, 074021

# $\pi$ and $K$ Form Factors : Probing the Standard Model



A. Miramontes, AB, K. Raya, P. Roig, Phys. Rev. D 105 (2022) 7, 074013

**Radial excitations of  $\pi$  and  $K$ :**

A. Miramontes, et. al. in preparation (Preliminary)

$$a_\mu^{\pi_1\text{-box}} = (-3.2 \pm 0.6) \times 10^{-13}$$

$$a_\mu^{K_1\text{-box}} = -6.8 \times 10^{-14}$$

$$a_\mu^{K^+\text{-box,DSE}} = -0.48(2) \times 10^{-11}$$

Eichmann, et. al. Phys.Rev.D 101 (2020) 5, 054015

Dispersive methods:

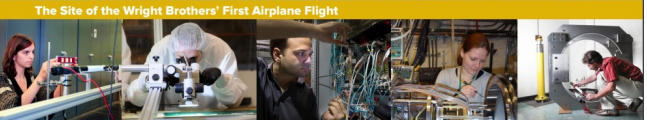
$$a_\mu^{\pi\text{-box}} = -15.9(2) \times 10^{-11}$$

$$a_\mu^{K^+\text{-box,VMD}} = -0.50 \times 10^{-11}$$

$$a_\mu^{\pi^\pm\text{-box}} = -(15.6 \pm 0.2) \times 10^{-11}$$

$$a_\mu^{K^\pm\text{-box}} = -(0.48 \pm 0.02) \times 10^{-11}$$

# $\pi$ Form Factor at Large $Q^2$



REACHING FOR THE HORIZON

The Site of the Wright Brothers' First Airplane Flight

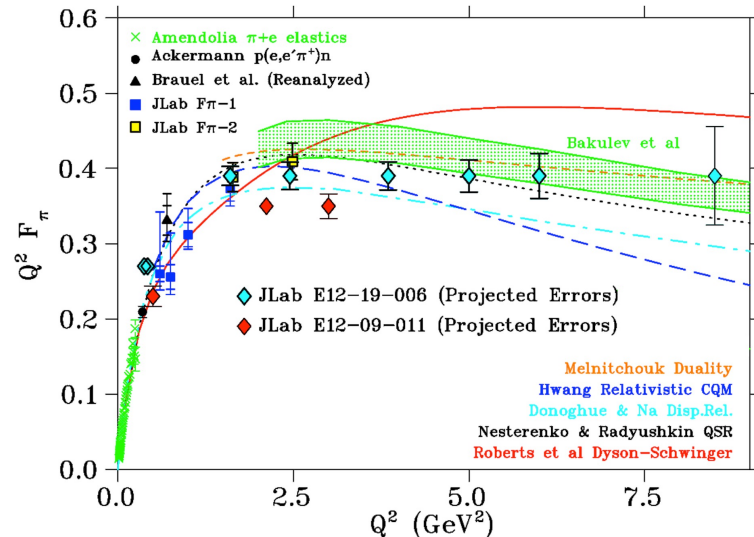
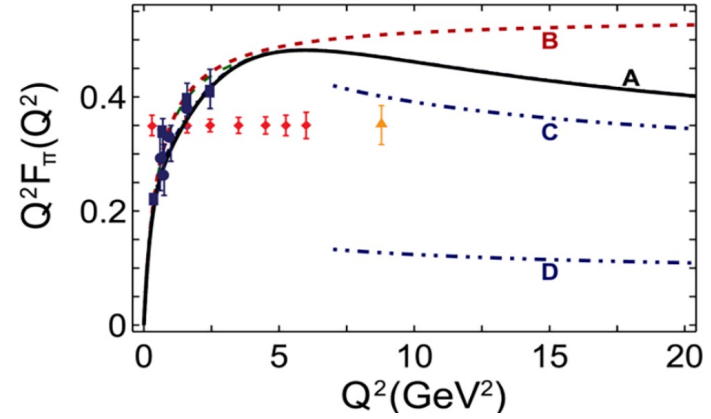
The 2015  
LONG RANGE PLAN  
for NUCLEAR SCIENCE



The study of the **pion form factor** is one of the **flagship goals** of the **JLab 12-GeV upgrade**... regime in which the phenomenology of **QCD** begins a **transition** from **large-** to **short-distance** scale behavior.

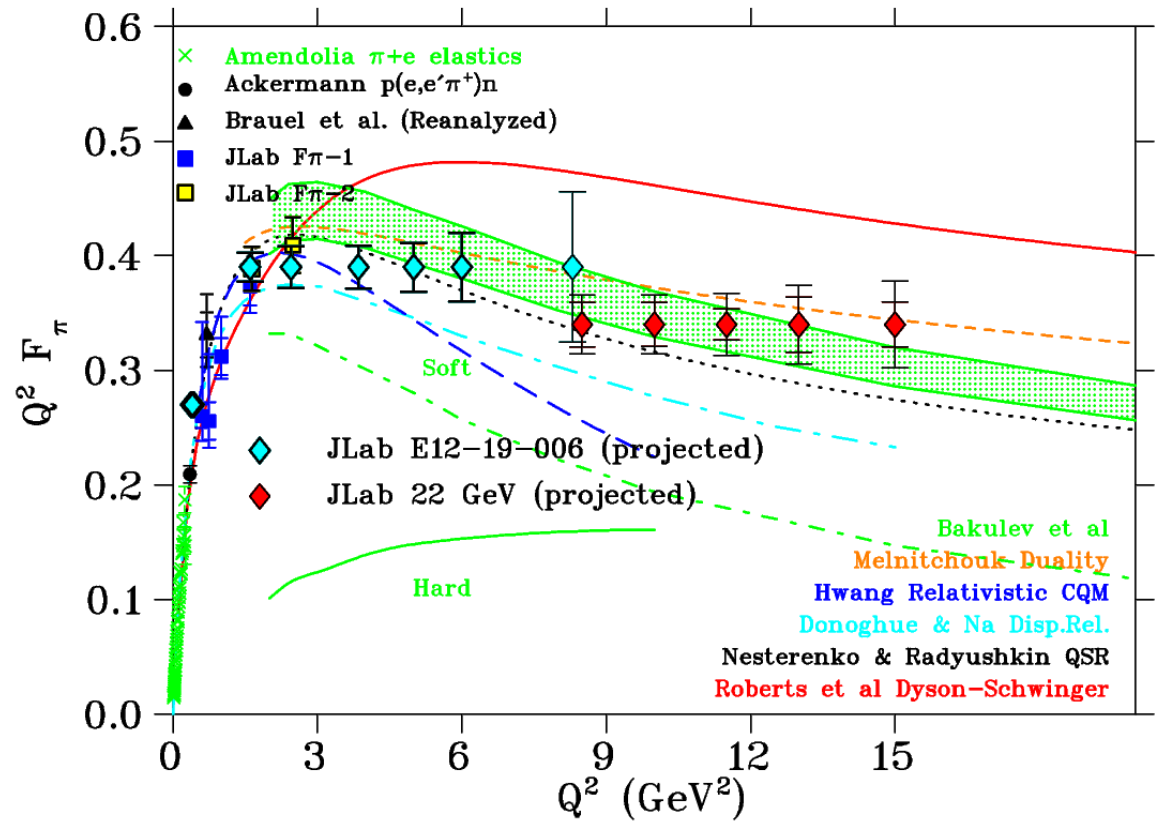
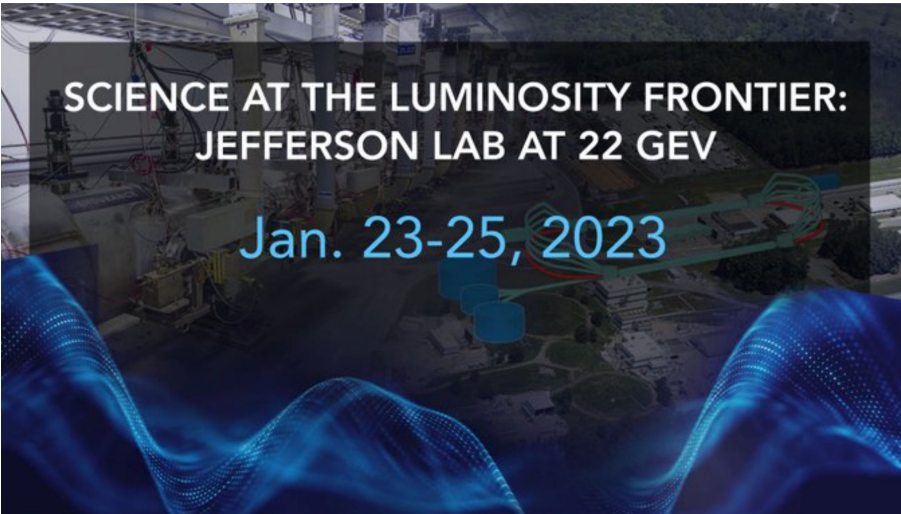
The **pion form factor** can potentially be measured till  **$Q^2 \sim 6-8$**  in the **12 GeV** upgrade of the **JLab**.

Courtesy Garth Huber



# $\pi$ Form Factor at Large $Q^2$

With a potential and desirable next **22-GeV** upgrade of the **JLab**, the **pion electromagnetic form factor** could be measured till  **$Q^2 \sim 15 \text{ GeV}^2$** .



Courtesy Garth Huber

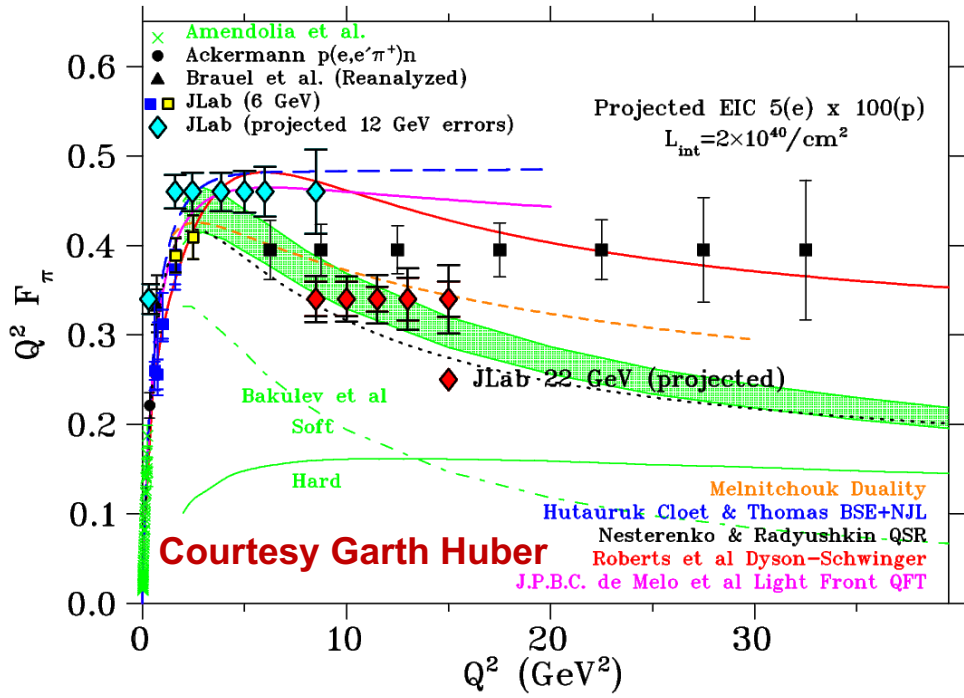
# $\pi$ and K Form Factor at Large $Q^2$

**Science Question:** Can we get quantitative guidance on the **emergent pion mass** mechanism?

**Key measurement:** **Pion form factor** data for  **$Q^2$ : 10-40  $\text{GeV}^2$** .

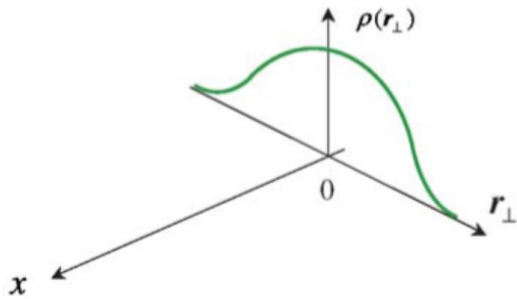
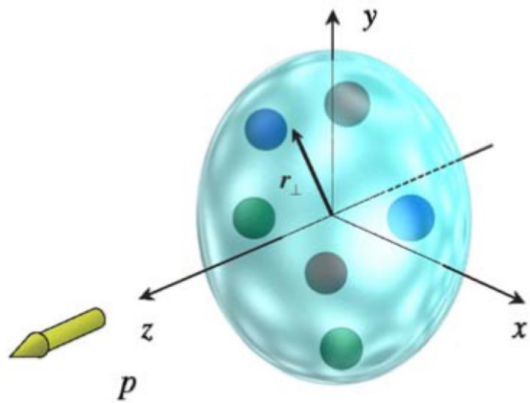
**Science Question:** How much interference is between emergent and Higgs mass mechanism?

**Key measurement:** **Kaon form factor** data for  **$Q^2$ : 10-20  $\text{GeV}^2$** .

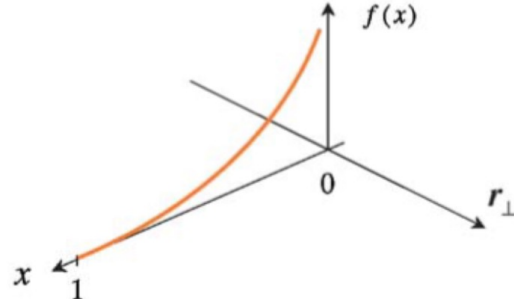
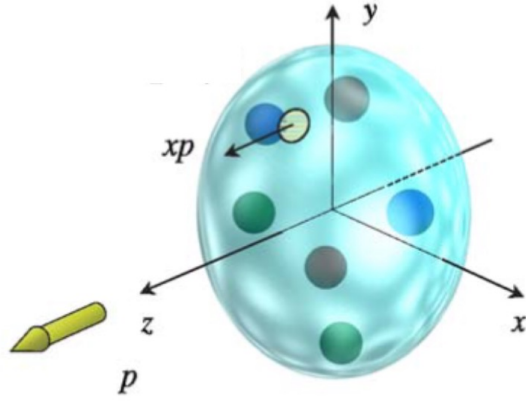




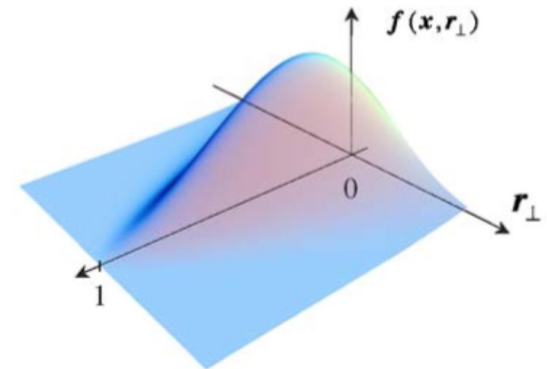
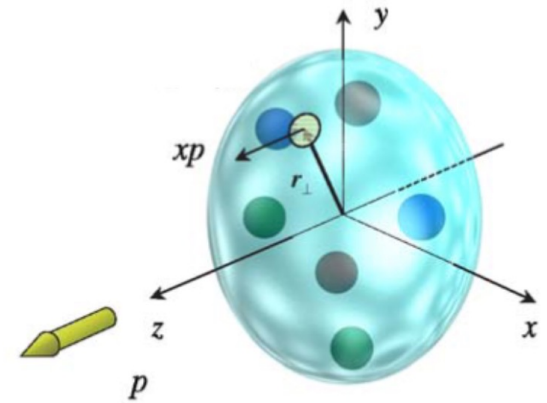
# $\pi$ and $K$ : Towards a 3-Dimensional Picture



Fourier transform of the elastic form factor



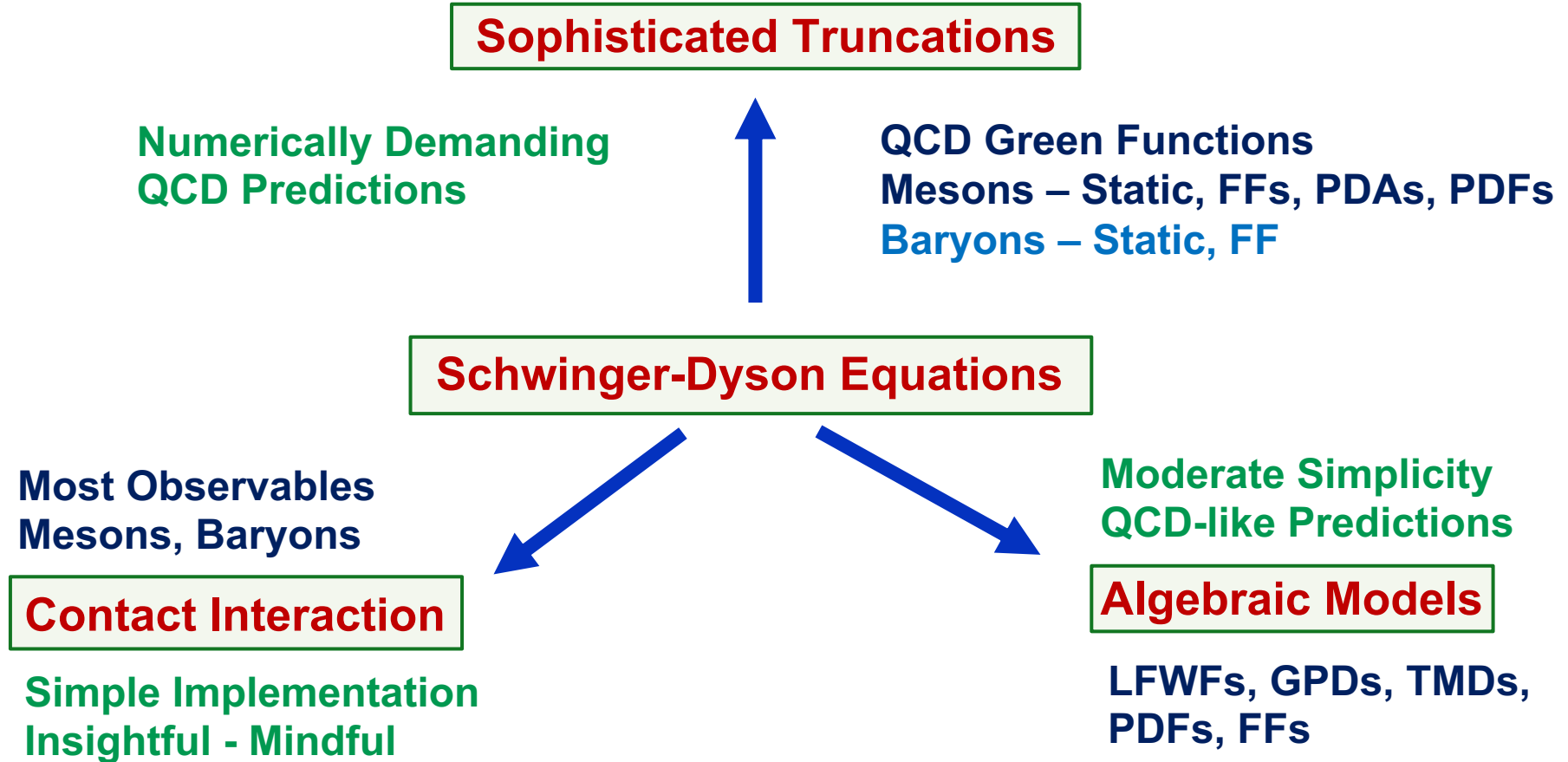
Parton Distribution



Skew-less Generalized Parton Distribution

# Towards Algebraic Models

---



# The Algebraic Model (AM)

- It retains the **constant term** from original models, setting it to  $\mathbf{M}_q$ .
- There is a **term linear** in  $\mathbf{w}$  with the coefficient  $(\mathbf{M}_h^2 - \mathbf{M}_q^2)$ . For same **flavored quarks**, it ceases to contribute by construction.
- There is a **quadratic term  $\mathbf{w}^2$**  with coefficient  $\mathbf{m}_M^2$ . The condition

$$|M_{\bar{h}} - M_q| \leq m_M \leq M_{\bar{h}} + M_q$$

- It guarantees the **positivity** of

$$\Lambda^2(w)$$

## The quark propagator:

$$S_{q(\bar{h})}(k) = [-i\gamma \cdot k + M_{q(\bar{h})}] \Delta(k^2, M_{q(\bar{h})}^2)$$

$$\Delta(s, t) = (s + t)^{-1}$$

## Bethe-Salpeter Amplitude:

$$n_M \Gamma_M(k, P) = i\gamma_5 \int_{-1}^1 dw \rho_M(w) [\hat{\Delta}(k_w^2, \Lambda_w^2)]^\nu$$

$$\hat{\Delta}(s, t) = t\Delta(s, t), \quad k_w = k + (w/2)P$$

$M_{q(\bar{h})}$  is constituent quark mass for a given flavor

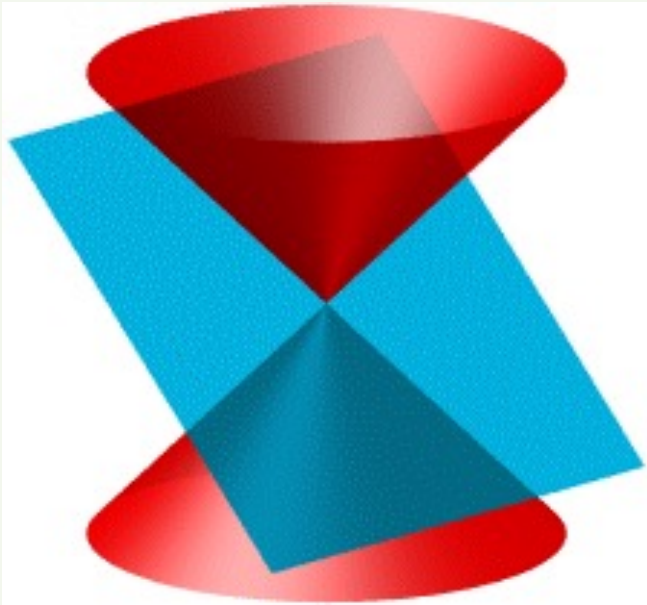
$n_M$  is a normalization constant

$\rho_M(w)$  is a spectral density

$$\Lambda^2(w) = M_q^2 - \frac{1}{4}(1 - w^2)m_M^2 + \frac{1}{2}(1 - w)(M_{\bar{h}}^2 - M_q^2)$$

# The Light Front Wavefunction

For a quark in pseudo-scalar meson **M**, the **leading twist** (2-particle) **light front wave function**,  $\psi_M$ , can be obtained via the light front projection of the meson's **BSWF**.



**Bethe-Salpeter Wavefunction:**

$$\chi_M(k, P) = S_q(k + P/2) \Gamma_M(k, P) S_{\bar{h}}(k - P/2)$$

**Light Front Wavefunction:**

$$\psi_M^q(x, k_{\perp}^2) = \text{tr} \int_{dk_{\parallel}} \delta(n \cdot k - x n \cdot P) \gamma_5 \gamma \cdot n \chi_M(k - P/2, P)$$

$$n \text{ lightlike, } n^2 = 0 \text{ and } n \cdot P = -m_M$$

**BSA:**

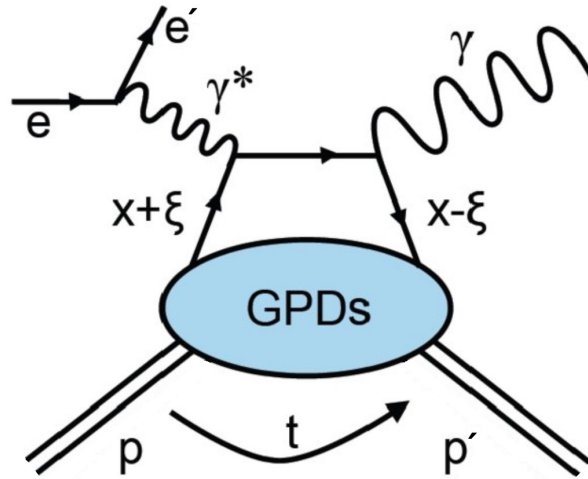
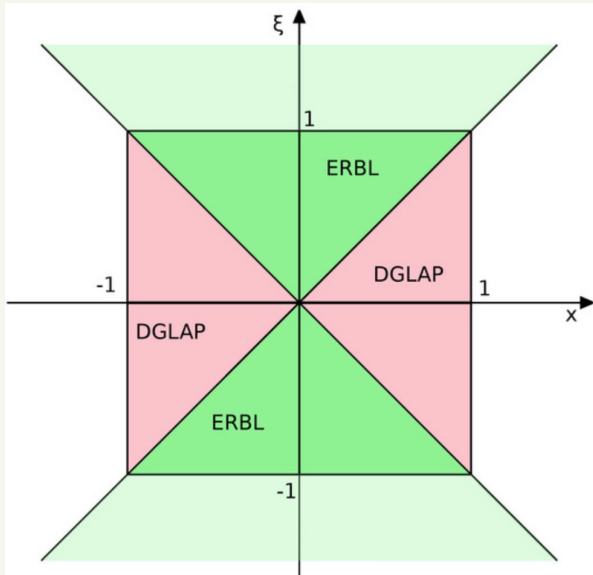
$$f_M \phi_M^q(x) = \frac{1}{16\pi^3} \int d^2 k_{\perp} \psi_M^q(x, k_{\perp}^2)$$

**The Algebraic Model:**

$$\psi_M^q(x, k_{\perp}^2) = 16\pi^2 f_M \frac{\nu \Lambda_{1-2x}^{2\nu}}{(k_{\perp}^2 + \Lambda_{1-2x}^2)^{\nu+1}} \phi_M^q(x)$$

# The GPDs from the overlap representation

Valence quark **GPD** from the overlap representation of the **LFWF**.  
 Both  $x$  and  $\xi$  have support on  $[-1, 1]$ .  
 The overlap representation is only valid in the **DGLAP** region,  $|x| > \xi$ .



$$P = (p + p')/2$$

$$-t = \Delta^2 = (p - p')^2$$

$$x = \frac{n \cdot k}{n \cdot P}$$

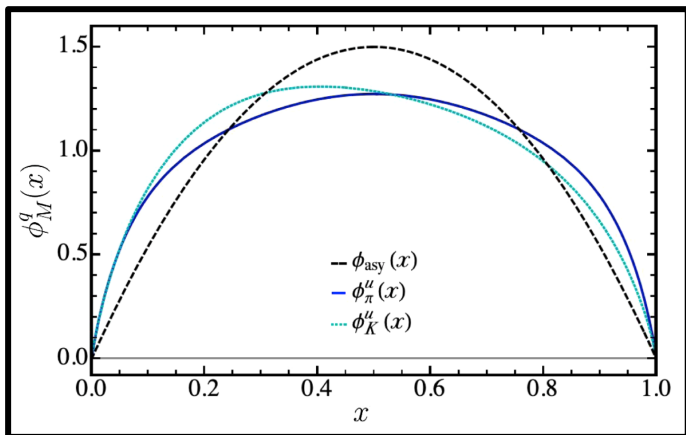
$$\xi = -\frac{n \cdot \Delta}{2n \cdot P}$$

$$H_M^q(x, \xi, t) = \int \frac{d^2 k_\perp}{16\pi^3} \psi_M^{q*}(x^-, (\mathbf{k}_\perp^-)^2) \psi_M^q(x^+, (\mathbf{k}_\perp^+)^2)$$

$$x^\pm = \frac{x \pm \xi}{1 \pm \xi} \quad \mathbf{k}_\perp^\pm = k_\perp \mp \frac{\Delta_\perp}{2} \frac{1 - x}{1 \pm \xi}$$

$$\Delta_\perp^2 = \Delta^2(1 - \xi^2) - 4\xi^2 m_M^2$$

# From the PDAs to the LFWFs



**$\pi$  and  $K$  PDAs**

Z.-F. Cui, et. al.,  
Eur. Phys. J. C 80, 1064 (2020).

$$(\bar{x} = 1 - x)$$

$$\phi_{\pi}^u(x) = 20.226 x \bar{x} [1 - 2.509 \sqrt{x \bar{x}} + 2.025 x \bar{x}]$$

$$\phi_K^u(x) = 18.04 x \bar{x} [1 + 5x^{0.032} \bar{x}^{0.024} - 5.97x^{0.064} \bar{x}^{0.048}]$$

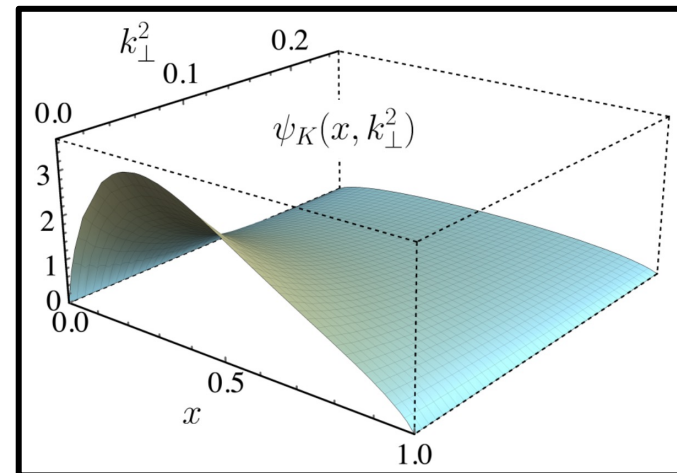
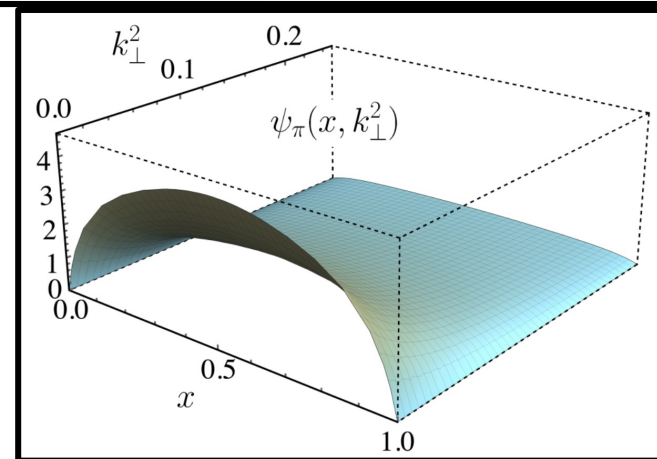
Drawing upon accumulated information on the **PDAs** of  $\pi$  and  $K$ , we parameterize them as corrections to the asymptotic PDA form on the hadronic scale.

**LFWF**  $\psi_M^q(x, k_{\perp}^2)$

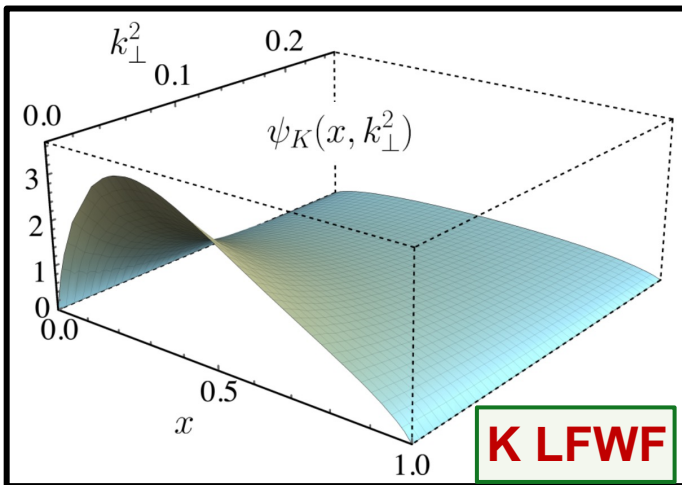
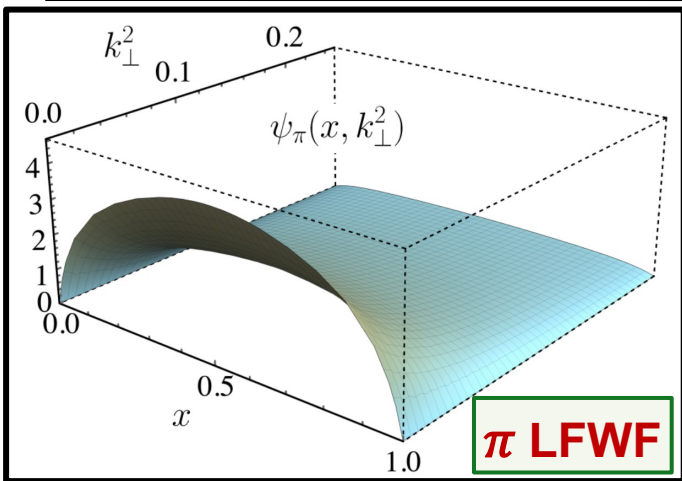



**PDA**


$$\frac{16\pi^2 f_M \nu \Lambda_{1-2x}^{2\nu}}{(k_{\perp}^2 + \Lambda_{1-2x}^2)^{\nu+1}} \phi_M^q(x)$$



# From the LFWFs to the GPDs



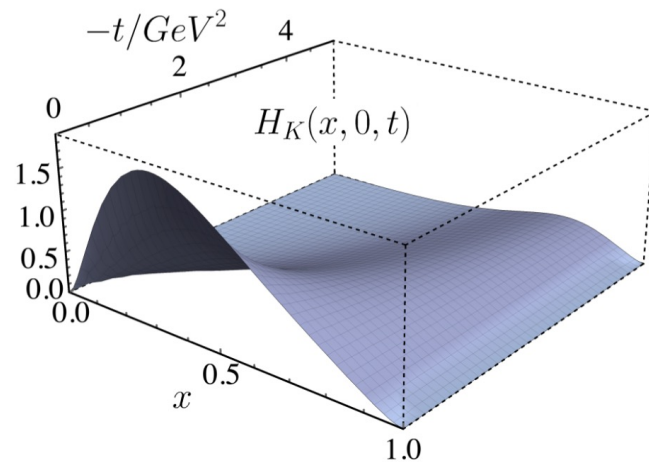
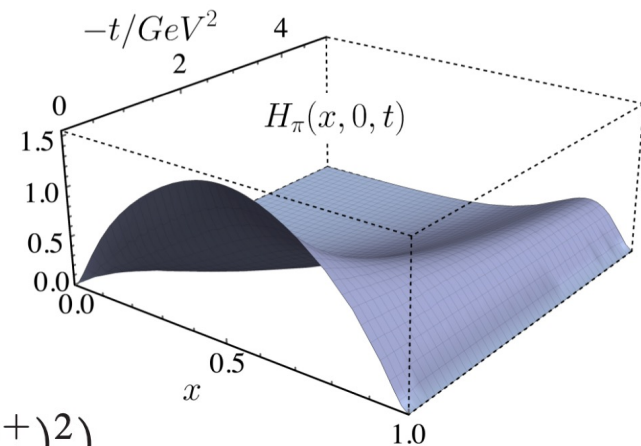
  
 $H_M^q(x, \xi, t)$

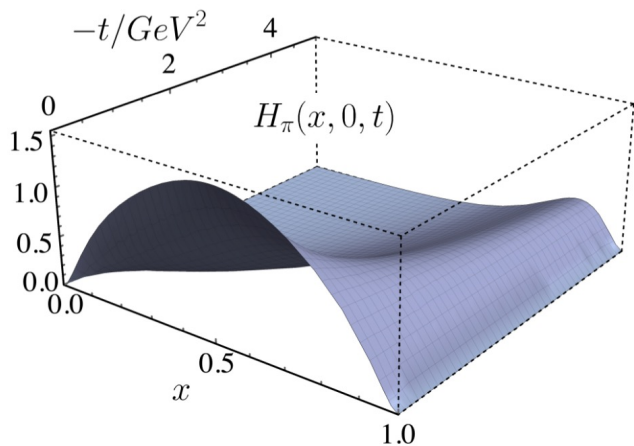
$$\int \frac{d^2 k_\perp}{16\pi^3} \psi_M^{q*}(x^-, (\mathbf{k}_\perp^-)^2) \psi_M^q(x^+, (\mathbf{k}_\perp^+)^2)$$

Overlap Representation  
of the GPDs

L. Albino, M. Higuera, K. Raya, AB  
Phys. Rev. D 106 (2022) 3, 034003



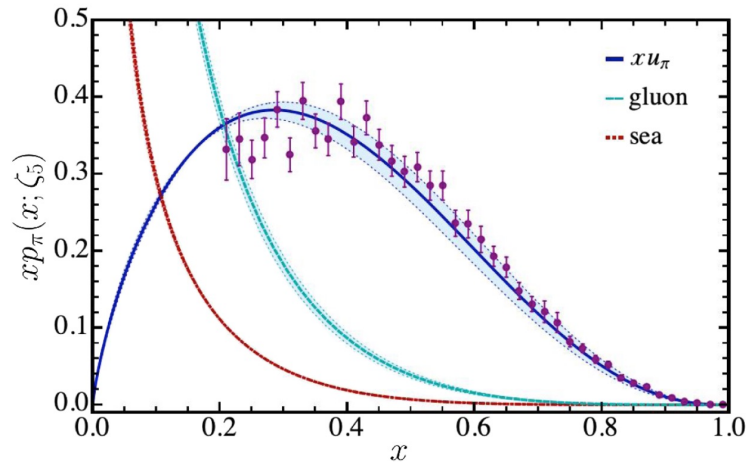
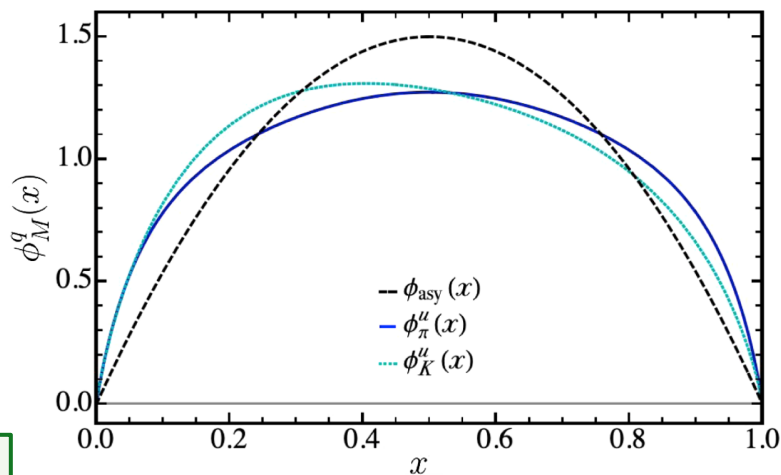
# From the GPDs to the PDFs



$$q_M(x) \equiv H_M^q(x, 0, 0)$$

**DGLAP Evolution  
Equations**

L. Albino, M. Higuera, K. Raya, AB  
Phys. Rev. D 106 (2022) 3, 034003

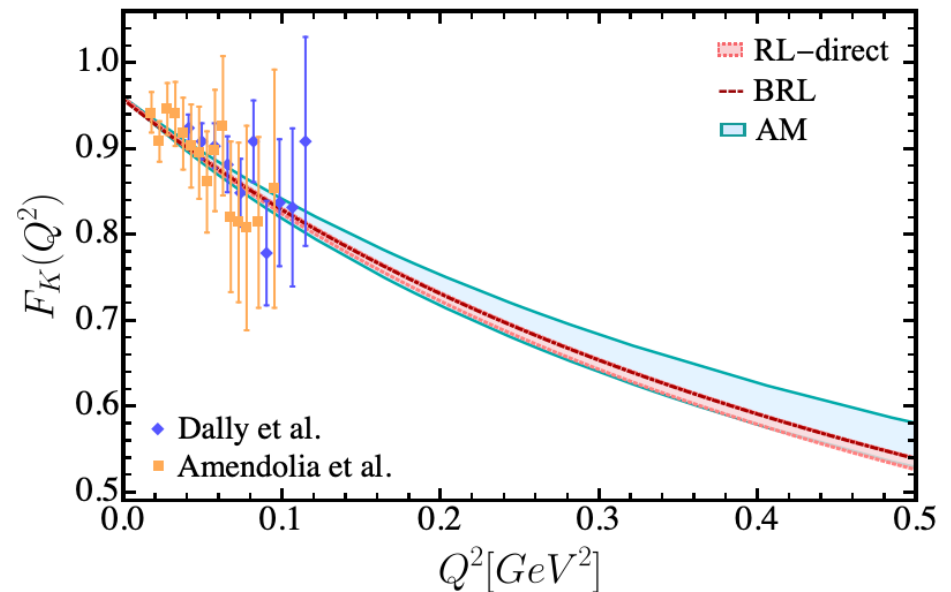
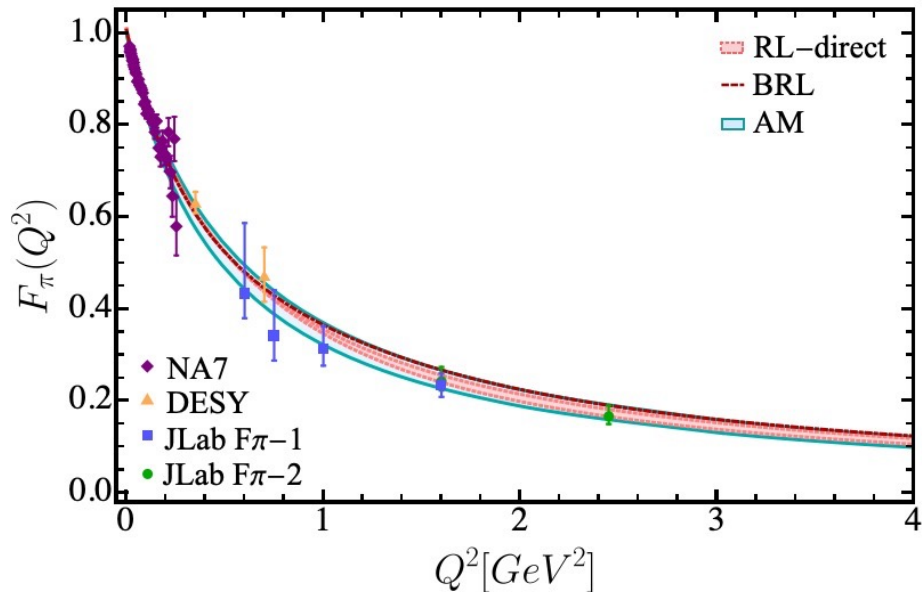




# Completing the Cycle – Back to Form Factors

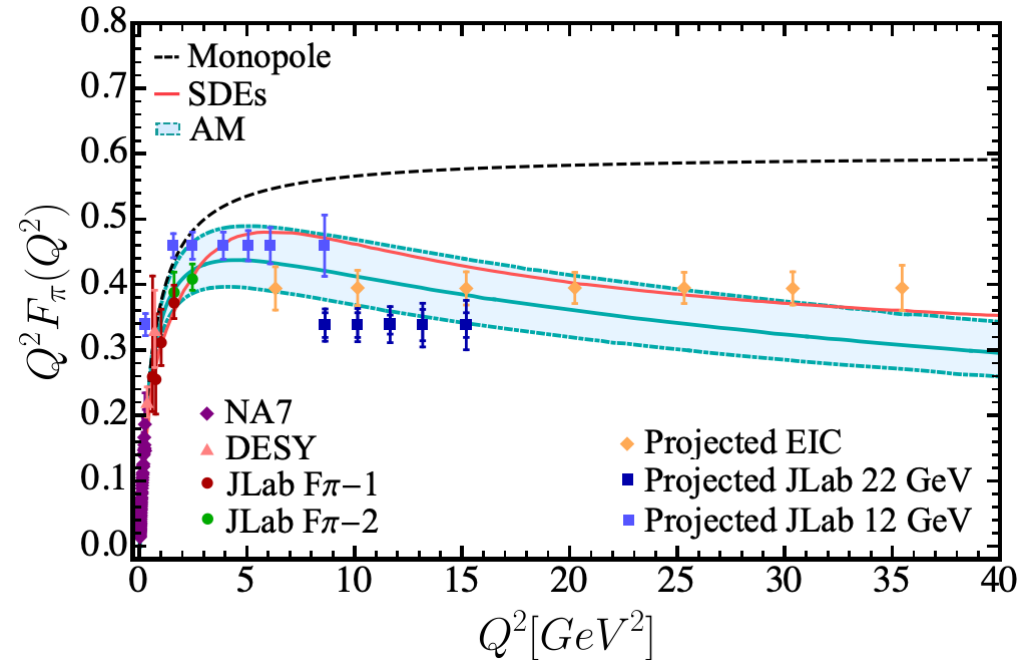
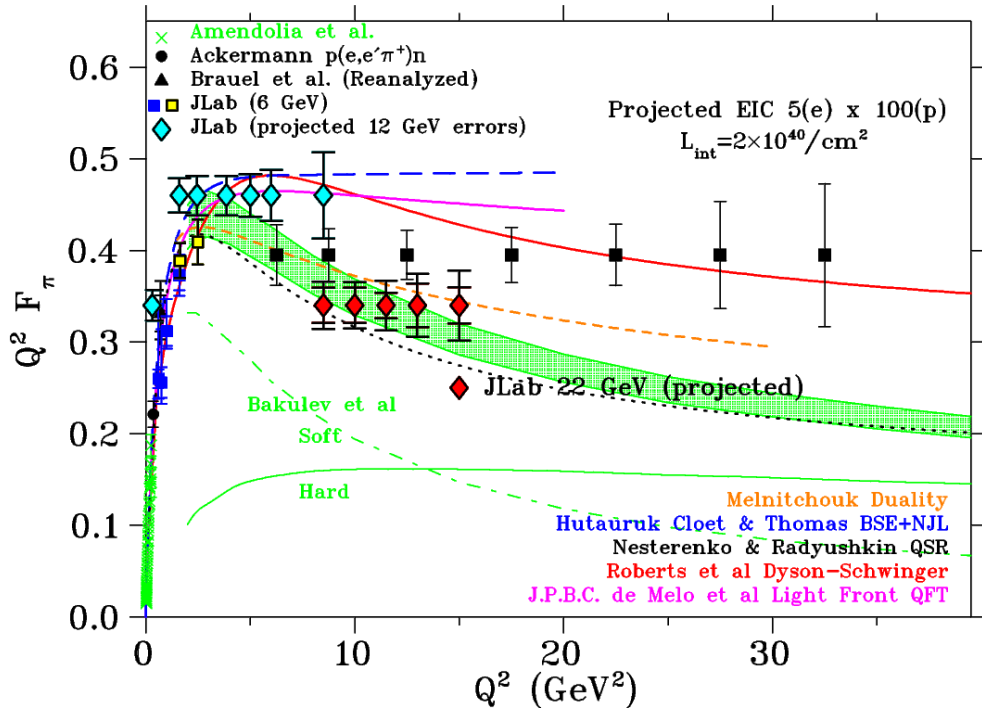
The **electromagnetic form factors** using our **algebraic model** can be obtained either through the knowledge of the **GPDs** or the direct evaluation of the **triangle diagram**.

Such an exercise provides stringent constraints on the efficacy of the **algebraic model** we have constructed by direct comparison with the refined calculation of these **form factors**.



# Completing the Cycle – Back to Form Factors

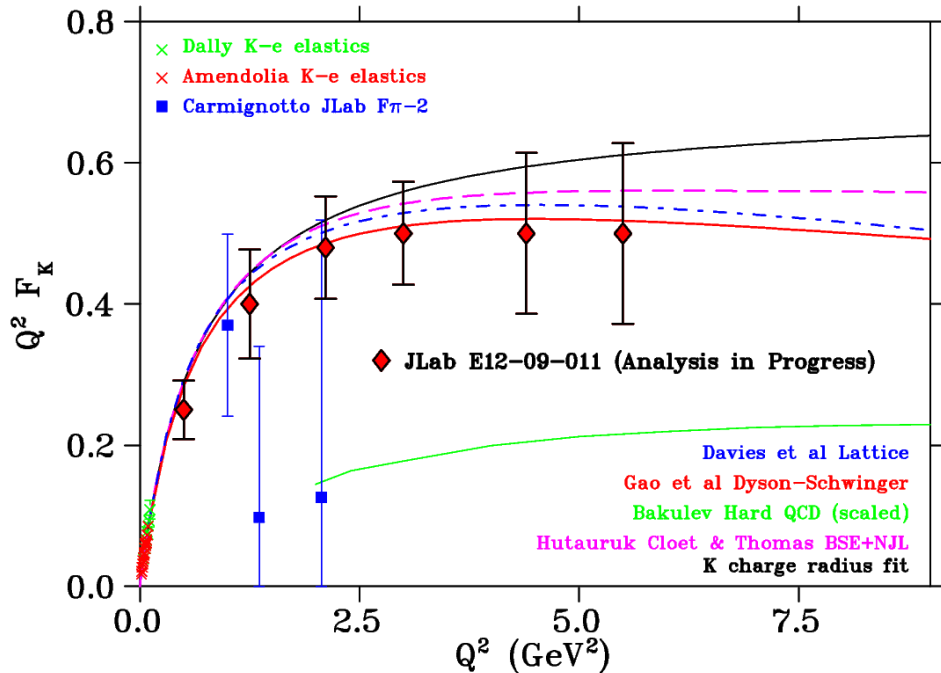
We can extend this analysis of the **Algebraic Model** to compute the **pion electromagnetic form factors** to larger  $Q^2$  range: **0-40 GeV<sup>2</sup>** which would likely cover the photon virtualities accessible to the **JLab12, JLab22** and **EIC programs**:



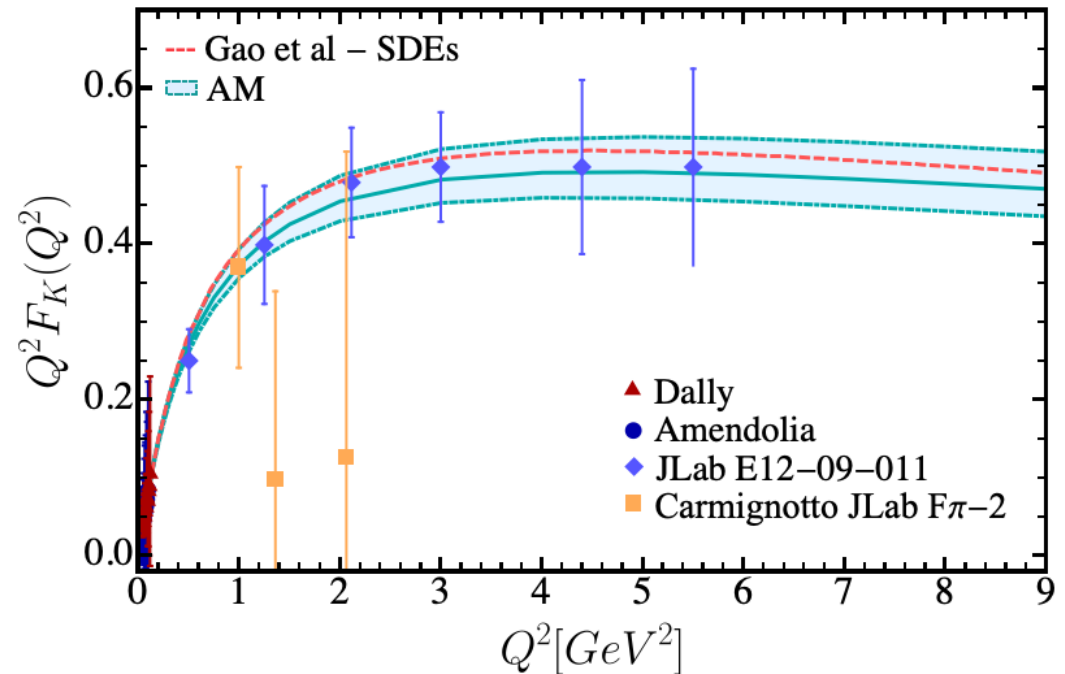
# Completing the Cycle – Back to Form Factors

There is an analysis underway of the **kaon electromagnetic form factor** till **5.5 GeV<sup>2</sup>** of the data obtained in **JLab E12-09-011** experiment.

Courtesy Garth Huber



Algebraic Model results



# Summary and Outlook

---

- The interplay of **QCD akin** truncations of **Schwinger-Dyson equations** and **algebraic model** based upon these studies shed important light on the **internal structure** of **pion** and **kaon**.
- **QCD akin** refined computation of **pion** and **kaon electromagnetic form factors** at low and intermediate virtualities of the probing photon in electroproduction processes:

A. Miramontes AB, K. Raya, P. Roig, Phys. Rev. D 105 (2022) 7, 074013

L. Chang, I.C. Cloët, C.D. Roberts, S.M. Schmidt, P.C. Tandy, Phys. Rev. Lett. 111 (2013) 14, 141802

- Results for the **pion electromagnetic form factor** at large photon virtualities accessible to the potential **22GeV upgrade** of the **JLab** and **EIC** are also available:

L. Chang, I.C. Cloët, C.D. Roberts, S.M. Schmidt, P.C. Tandy, Phys. Rev. Lett. 111 (2013) 14, 141802

J. Arrington, et al. (Feb 23, 2021, J.Phys. G 48 (2021) 7, 075106

- More recently, **pion** and **kaon form factors** have been computed in the the **time-like region**

A.S. Miramontes, H. Sanchis Alepuz, R. Alkofer, Phys. Rev. D 103 (2021) 11, 116006

A.S. Miramontes, AB, Phys. Rev. D 107 (2023) 1, 014016

# Summary and Outlook

---

- Carefully constructed **Algebraic Models** can enable computation of the **GPDs**, **PDFs** and **EFF** with relative ease which is reminiscent of a **contact interaction** while mimicking the reliability of **QCD akin** refined truncations of **Schwinger-Dyson equations**.

L. Albino, M. Higuera, K. Raya, AB Phys. Rev. D 106 (2022) 3, 034003

- Despite these encouraging results and synergy with experimental endeavors at **JLab** and **EIC**, further improvements and extensions in the **continuum QCD approach** are desirable.
- Deeper research into the theoretical foundations of the truncations involved at the level of the **Green functions** of the fundamental degrees of freedom, i.e., **quarks**, **gluons**, as well as **quark-gluon** and **gluon-gluon** interactions continues vigorously.
- **Schwinger-Dyson equations** have also been of substantial success in the studies of **baryons** such as the **transition form factors** of **nucleon** to its **excited states** which is a hallmark of **CLAS**, **CLAS12** and **CLAS22** programs at **JLab** and hold the promise to offer a reliable tool for the future **JLab** and **EIC era** research into the heart of **hadronic matter**.

$N \rightarrow N^*(1520)$  Transition Form Factors

**Thank you for your attention**